Comparing the Accuracy of Unmanned Aerial Vehicles and Ground Surveying Methods for Road Corridor Surveys: A Case Study of Parkoso Road

B. O. Asamoah Asante[1], Y. M. Asare [2], J. A. Danquah[1], E.K. Larbi[1], O. Kwarteng[1]
[1] Geo-Informatics Division, Building and Road Research Institute (CSIR-BRRI), Kumasi, Ghana
[2] Department of Geomatic Engineering, Kwame Nkrumah University of Science and Technology (KNUST)
*Corresponding author email: padomiski@gmail.com

(Received on 03 March 2024; In final form on 02 September 2025)

DOI: *https://doi.org/10.58825/jog.2025.19.2.153*

Abstract: Traditional ground-based surveying methods in highway engineering often fall short in meeting project timelines because they are slow. Consequently, researchers are exploring new techniques to deliver accurate and reliable data within project schedules. However, these new approaches must demonstrate their reliability and effectiveness across various scenarios. This study aims to compare the accuracy of Unmanned Aerial Vehicles (UAVs) and Real-Time Kinematic GPS (RTK GPS) in road corridor surveys. The research utilizes two main datasets: the first records point positions and elevations along the corridor using RTK GPS, while the second includes geometrically corrected aerial photographs from UAV surveys. Ground Control Points (GCPs) are used as benchmarks to ensure comparable accuracy between RTK GPS and UAV data. Notably, minimal positional shifts were observed between the two methods. Longitudinal profiles and cross-sections derived from both datasets were overlaid, showing negligible differences. Root Mean Square Errors (RMSEs) were calculated as 0.025m, 0.041m, and 0.065m for Eastings, Northings, and Elevations, respectively. The Arithmetic Mean Error (AME) and the Arithmetic Mean Standard Error (AMSE) were 0.032m and 0.0795m. Additionally, the Arithmetic Standard Deviation (ASD) between the survey methods was 1.1615E-16m. These statistical results indicate a strong agreement between UAV and RTK GPS measurements, suggesting UAVs can provide sufficient accuracy comparable to RTK GPS for road corridor topographic surveys.

Keywords: Unmanned Aerial Vehicles, Ground Surveying, Road Corridor Surveys, Accuracy Comparison RTK GPS

1. Introduction

Road infrastructure is regarded as a vital element of any nation's social and economic progress (Ivanova and Masarova, 2013). It affects the flexibility and mobility of both the workforce and goods, which impacts employment levels (Papí Ferrando et al., 2007). The geographic information of areas is directly linked to a country's economic development and is even more connected to the creation of modernity (Shi and Wang, 2021). Surveys are conducted throughout the entire road construction process, from setting out road center lines to creating vertical and transverse sections (Wang and Hu, 2013). In addition to project design quality, the accuracy and precision of survey data are critical for transferring data from the field to the project (Moser et al., 2016). Organizational management and a lack of documentation detailing terms among collaborators remain major challenges in road surveys and construction (Bouziani et al., 2010). Highway engineers face the realization that traditional ground survey methods are too slow to meet deadlines without significantly increasing survey personnel (Pryor, 2004). This has drawn the attention of governments, planners, surveyors, engineers, geospatial professionals, and transport stakeholders to develop new, efficient surveying methods to meet future needs and facilitate improvements and innovations (Pryor, 2004). Land surveying has historically been used to gather information for the geometric design of roads, but the legal rules governing surveyor interventions do not specify survey requirements or surveyor duties within a road project. Due to weak enforcement of standards by government agencies and limited investment in the sector, protocols guiding surveyors' work are lacking, and there is little traceability of their activities (Bouziani et al., 2010). The current situation calls for the adoption of more effective surveying methods and procedures. Highway agencies responsible for overseeing and maintaining roads must set reliability standards for efficient highway surveying systems. The primary goal of road control measurements is to provide accurate guidance and elevation data for the survey, design, and construction lines. Horizontal and vertical data precision is especially important for structure stakeouts (Moser et al., 2016). The functional classification of roads, design speed, sizes and widths of all cross-section elements (lanes, medians, edge strips, shoulders), horizontal alignment design elements (tangents, transition curves, circular arcs), their physical parameters (radii, etc.), super elevation rates, and runoff must all be determined by a comprehensive road surveying system (Psarianos and Nakos, 2001). New ideas and methods are being explored to provide precise and reliable data within project timelines, but they must first pass tests of feasibility, adaptability, reliability, universality, and cost-effectiveness before being widely adopted in highway engineering and road surveys (Pryor, 2004).

An increasing number of engineering projects, surveys, and intelligent technologies depend on current, accurate geographic data (Park and Um, 2019). Since traditional methods often fall short of current demands, integrating new spatial data

collection technologies is necessary. This integration must be carefully evaluated to ensure comparable accuracy to conventional techniques (Lee et al., 2020). Modern survey methods are being developed in response to trends in geodetic science, emphasizing high precision and reliable data with minimal material and time costs (Moser et al., 2016). UAV photogrammetry has become prominent as a quick, low-cost, adaptable method for creating orthophotomosaics, point clouds, and 3D models of topographic features (Julge et al., 2019). Technological advancements have enabled UAVs to acquire measurements needed for road design (Zulkipli and Tahar, 2018).

Various surveying techniques—such as geodetic survey, GPS, levels, theodolites, total stations, and digital cadastral plans (DCP)—have been used to gather parameters like road width and topography, which are essential in design. Geodetic survey data serve as fundamental inputs for road development, offering high accuracy and detailed information, such as digital maps or plans (often digital cadastral plans - DCP) and topographic surveys (Ljutić et al., 2008). The pace of road development will accelerate significantly alongside growing urbanization, increasing the demand for precise and detailed road data (Wang and Hu, 2013). Digital cadastral plans, created by scanning analog maps into digital formats and vectorizing them, cannot be enhanced simply by increasing resolution or detail (Paar et al., 2010). DCPs often lack terrain elevation data and sufficient points for high-quality road planning. Using field survey data to correct parcel boundaries in digital cadastral surveys can greatly improve accuracy, especially in urban areas (Moser et al., 2016). However, traditional road surveying methods—such as GPS, levels, theodolites, total stations, and DCP—suffer from inconsistency, high costs, and time-consuming procedures (Li et al., 2020). Total stations measure horizontal and vertical angles as well as slope distances, making them widely used in engineering surveys and construction (Shi and Wang, 2021). They can locate points with an accuracy of about 1 cm (Beshr and Abo-Elnaga, 2001). The reflectivity and color of surfaces influence laser energy reflection, affecting measurement accuracy, especially at longer distances where errors increase (Beshr and Abo-Elnaga, 2001). Intervisibility and station relocation pose challenges in complex terrains (Wang and Hu, 2013). GPS surveying began in the 1980s, with post-processing being a major limitation. Even with modern equipment, local displacement can occur, making relative positioning within a single survey more accurate (Moser et al., 2016). RTK (Real-Time Kinematic) methods, introduced in the early 1990s, provide centimeter-level real-time positioning (Rizos, 2003). RTK is widely used for line measurement but requires base stations; accuracy diminishes with increased distance, with an effective range of about 15 km (Wang and Hu, 2013). Currently, surveyors often combine GNSS and robotic total station techniques for earthworks, road surveys, and layout tasks. Traditional surveys, though straightforward, are tedious and prone to omission errors due to surface irregularities between points (Julge et al., 2019). Modern methods such as Mobile Laser Scanning (MLS), satellite positioning, laser profiling, Mobile Mapping Systems (MMS), Ground Penetrating Radar (GPR), UAVs, and LiDAR are gaining popularity over traditional approaches (Li et al., 2020). MMS facilitates rapid and precise HD mapping (Um and Yong, 2021). MLS measures road surfaces in three dimensions, capturing longitudinal profiles, though data processing is intensive and often offline due to high computational demands (Li et al., 2020). LiDAR emits rapid laser pulses to measure surface distances, useful in road inventory mapping (Guan et al., 2016). UAV photogrammetry has become increasingly cost-effective for mapping long, narrow features like roads, thanks to advances in remote sensing technology, particularly UAV systems (Pajares, 2015). Despite its benefits, UAV surveying faces issues such as turbulence from strong thermal winds causing blurry images and safety concerns in populated areas (Cho et al., 2022). Nevertheless, its low cost, high speed, maneuverability, and safety have spurred research into its application for road surveys (Saadatseresht et al., 2015). UAV aerial photographs are geometrically corrected and mapped similarly to topographical maps, accurately showing ground locations which aid field engineers in measuring distances, areas, and terrain features directly (Siebert and Teizer, 2014). Both ground and UAV surveying methods have proven effective in solving road design challenges. Notable applications include digitization in road construction using UAVs (Winter et al., 2022), boundary verification (Chio and Chiang, 2020), road monitoring (Julge et al., 2019), road asset management with vehicle-mounted laser systems (Li et al., 2020), road inventory with mobile LiDAR (Guan et al., 2016), automated surface measurement with 3D laser sensors (Laurent et al., 2012), and GNSS RTK surveys (Moser et al., 2016). In Ghana, UAVs have been employed for various tasks like encroachment surveys and base map creation, though their use in road surveying remains limited due to the lack of detailed data on achievable accuracy and costs (Streiter and Wanielik, 2013). This study seeks a fast, accurate, and reliable measurement system for high-precision road data collection. To advance understanding and applicability, a comparative accuracy analysis of common ground surveying methods (GNSS RTK) and new technologies (UAV-drones) is presented.

2. Study Area

Parkoso, a suburb in the Ashanti Region, is situated in the northeastern part of the region between latitudes 06°43' N and 06°42' N and longitudes 01°33' W and 01°31' W. It falls within the Asokore Mampong Municipal Assembly, which borders Ejisu Juaben district to the east, Kwabre East to the north, Atwima district to the west, and Bosomtwe Kwanwoma district to the south. The municipality covers a total land area of 23.91 km² (Osman et al., 2018). The suburb experiences a tropical bi-modal rainfall pattern within a wet semi-equatorial climate (Amoah et al., 2012). The double maxima rainfall regime is approximately 214.3 mm in June and 165.2 mm in September (Acheamfour and Tetteh, 2014). The average minimum temperature is about 21.5°C, and the average maximum temperature is around 30.7°C; humidity levels average 84.16% at sunrise and 60% at sunset (Mensah et al., 2018). The study area is mainly

underlain by middle Precambrian rocks; it features two primary lithostratigraphic / lithotectonic complexes: Paleoproterozoic supracrustal and intrusive rocks, and Neoproterozoic to early Cambrian platform sediments, with elevations ranging from 250 to 300 meters above sea level (Osei-Nuamah and Appiah-Adjei, 2017). The area is located in the wet, semi-deciduous South-East Ecological Zone, specifically within the transitional forest zone (Acheamfour and Tetteh, 2014; Amoah et al., 2012). Additionally, the area's unique geological structure has contributed to the growth of the construction industry here (Osei-Nuamah and Appiah-Adjei, 2017). Figure 1 shows the route location used for the study.

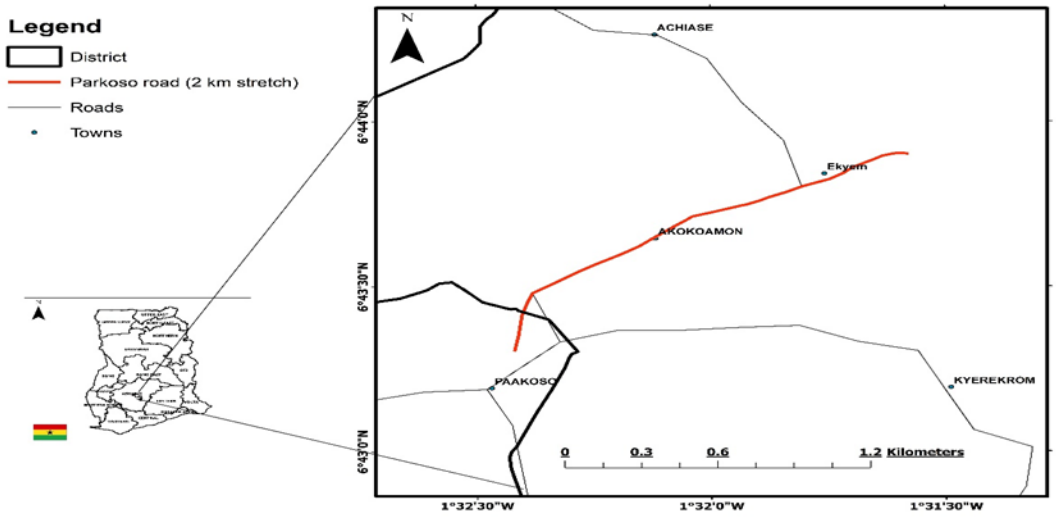

Figure 1. Map of Study Area

3. Resources and Methods Used

3.1 Resources

Two sets of primary data were collected for the study. The first set of data consists of the positions and elevations of points collected at the edges and centre points of the road corridor with the FOIF GNSS equipment in Real-Time Kinematic mode. The second set of data is made up of aerial photographs that were taken with the Mavic 2 Pro drone.

3.2 Software Used

The software used for processing and analyzing the field data are as follows:

i. Topcon Tools v 8.2.3
ii. Microsoft Excel 2016
iii. Agisoft Metashape v 1.7.6
iv. Quantum GIS v 3.28.0

3.3 Methods

A reconnaissance was done at the study area on to get an overview of the study area. A location with a clear line of sight to the sky in all directions was chosen within the study area for the establishment of a temporary benchmark to be used as the base station for the Real-Time Kinematic GPS equipment that was used for the topographic survey of the road corridor. The rover of the GPS equipment was then set up on the temporary benchmark and made satellite observations for 37 minutes. The raw data was afterwards downloaded and post-processed to obtain the coordinates and elevation of the benchmark. The GNSS equipment was set up in Real-Time Kinematic mode with the base equipment set up on the benchmark. The rover was used to collect the positions and elevations of road edges, road centres, and other features within the road corridor at 25m intervals along the road. After using the RTK GPS for the topographic survey, markers were placed along the road at areas that will be visible to the drone when in flight. The positions and elevations of each of the markers were observed. A flight plan was then prepared with the Drone Deploy software, after which the flight was executed. The data from both surveying methods were downloaded, processed, analyzed and compared. Figure 2 is a flowchart that shows all the steps that were undertaken to achieve the final results.

3.4 Using RTK-GPS for the road corridor Survey

To initiate the Real-Time Kinematic GPS technique, an initial control point was established within the study area. This was achieved through the utilization of GNSS equipment in static mode, leveraging the Continuously Operating Reference Station (CORS) with UTM coordinates (741977.365N, 662688.938E, Z: 349.647) as the reference position. In the study area, a strategically chosen site with unobstructed sky visibility from all directions was designated, and a Temporary Benchmark was created. This Temporary Benchmark functioned as the foundational station for executing the Real-Time Kinematic ground surveying process.

The next step involved placing the Rover on the Temporary Benchmark in static mode, where it observed the benchmark's position for a duration of 37 minutes. Subsequent to these GPS observations, the raw data from both the base station and the rover were extracted and subjected to post-processing using the Topcon Tools Post-Processing Software. This entailed transforming the raw equipment data into the Receiver Independent Exchange (RINEX) format, which is the compatible format for the processing software

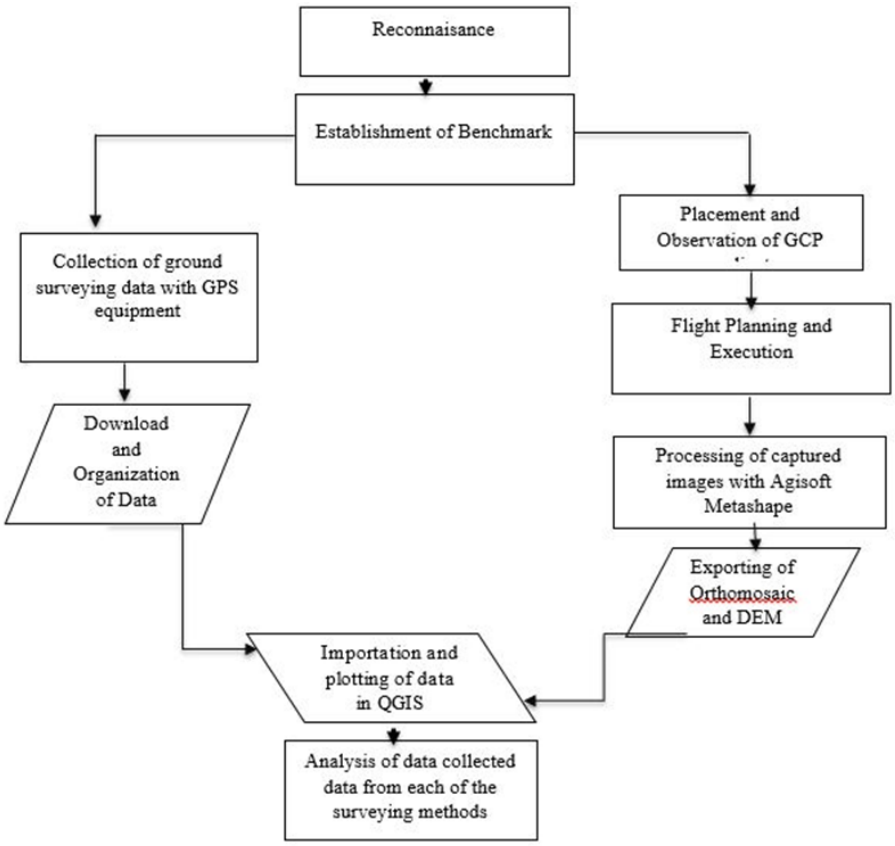

Figure 2. Flow Chart of Methodology

Upon obtaining the precise benchmark coordinates, the GNSS equipment's mode transitioned from Static to Real-Time Kinematic. The base equipment was positioned on the benchmark, and its coordinates and elevation were inputted into the logging system. This facilitated the establishment of a communication link between the base station and the rover, enabling real-time correction transmissions from the base station to the rover.

For the actual survey along the designated road, the road was segmented into intervals of 25 meters known as chainages, commencing from chainage 0+000 and extending to chainage 2+000. At each of these chainage points, comprehensive three-dimensional coordinates of both the road corridor boundaries and the road center were captured utilizing the Rover operating in RTK mode

3.5 Aerial Survey Process and Ground Control Point Establishment

For the aerial survey, the Mavic 2 Pro Unmanned Aerial Vehicle (UAV) was deployed to execute the flight. In order to ensure accurate georeferencing of the images captured by the drone, markers were strategically positioned along the road corridor. These markers, known as Ground Control Points (GCPs), played a vital role in the geospatial alignment of the acquired aerial imagery. In total, eleven GCPs were employed, with an average spacing of approximately one marker per 180 meters of road length.

To attain precise georeferencing, the RTK GNSS equipment was employed to record the coordinates and elevations of each individual Ground Control Point. This was achieved by leveraging an established benchmark serving as the base station, with coordinates 743564.78N, 661369.44E, Z: 361.158.

In Table 1, the coordinates and elevations of the Ground Control Points are presented, offering a comprehensive overview of the geospatial data collected.

Once the ground control points' coordinates were accurately recorded, the subsequent step involved devising a flight plan for the UAV. This flight plan was meticulously crafted using the Drone Deploy software, a tool designed to facilitate efficient and controlled drone flights for data acquisition purposes.

3.6 Creation of longitudinal Profile

Creating the longitudinal profile of the road corridor involved utilizing Microsoft Office Excel software, version ... The initial step entailed importing the road center points' elevations and corresponding chainages into the software. Subsequently, within the 'Insert' tab, a Line Chart was chosen as the visualization tool. The column housing the elevation data was designated for the vertical axis, while the column containing chainage information was designated for the horizontal axis. This process resulted in the generation of a line plot that effectively illustrates the elevation variations at different chainage points.

Table 1. Coordinates of Ground Control Points that were used for georeferencing

GCP	NORTHING	EASTING	ELEVATION
GCP1	743269.912	661257.399	323.726
GCP2	743569.094	661369.874	316.016
GCP3	744365.510	662638.808	327.010
GCP4	744382.102	662752.049	323.992
GCP5	744398.750	662856.832	317.038
GCP6	744219.437	662446.750	328.796
GCP7	744184.588	662283.370	324.872
GCP8	744079.884	662066.360	326.684
GCP9	743955.469	661904.983	335.264
GCP10	743854.156	661789.092	324.292
GCP11	743742.971	661607.690	312.551

4. Results

4.1 Using Real-Time Kinematic GPS for the road corridor topographic survey

After making the GPS observation on the temporary benchmark and post-processing the raw data, the coordinates obtained were 743564.78m N, 661369.44m E (in the WGS84 – UTM Zone 30N coordinate system) and an elevation of 361.158. Table 2 shows a sample of the field data collected with the RTK GPS when it was used for the topographic survey of the road corridor. It contains the Eastings, Northings, Elevations, and Descriptions of the points. It also contains the chainages within which each of the points falls. In addition, the table indicates the Horizontal Root Mean Square Error (HRMS) and the Vertical Root Mean Square Error (VRMS) for each observation. The minimum and maximum HRMS obtained for the observations were 0.008m (8mm) and 0.028m (28mm), respectively. For the VRMS of the observations, the minimum and maximum were 0.013m (13mm) and 0.029 m (29mm), respectively. Figure 3 shows the longitudinal profile of the road corridor as generated from the RTK GPS topographic survey data. The profile shows a maximum elevation of 335.461m and a minimum elevation of 309.975m.

The attainment of accuracy in the RTK GPS survey was meticulously executed through a series of protocols. Measurements were exclusively taken when the GPS achieved a "fix" status, ensuring optimal precision in the data collection process. By evading instances of a "float" status, which could potentially compromise the overall Root Mean Square Error (RMSE) accuracy, the survey integrity was preserved. Particularly in regions characterized by dense vegetation and structures along the road corridor, extended observation periods were applied to sidestep the occurrence of "float" status.

Furthermore, rigorous quality control measures were implemented to uphold an RMSE threshold of less than 0.05 meters. This involved configuring the GPS equipment to dismiss observations that surpassed the specified RMSE criterion. In-depth analysis of the RTK GPS survey data employed the arithmetic mean statistical indicator. This analysis was then benchmarked against the precision standards outlined by authoritative bodies such as the United States' National Standard for Spatial Data Accuracy (NSSDA) and the American Society for Photogrammetry and Remote Sensing (ASPRS).

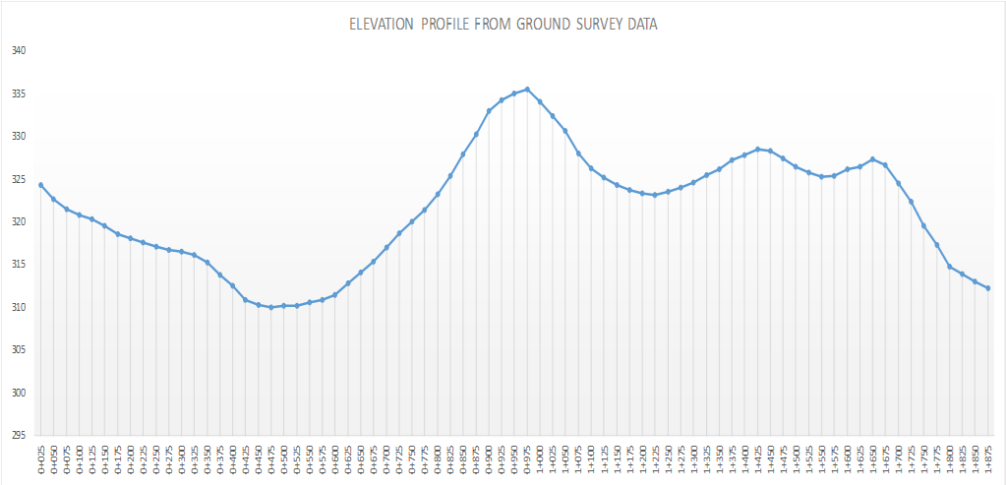

Figure 3. Longitudinal Profile of the road from the RTK GPS survey data

Table 2. A sample of results from the RTK GPS topographic survey

Point Name	Easting	Northing	Elevation	HRMS	VRMS	Code	Chainages
Pt1	661257.545	743251.427	324.082	0.009	0.017	RL	
Pt2	661261.292	743249.590	324.277	0.009	0.018	C	0+000
Pt3	661264.438	743247.948	324.574	0.010	0.019	RR	
Pt4	661266.774	743276.205	323.066	0.009	0.018	RL	
Pt5	661269.404	743275.140	322.668	0.010	0.021	C	0+025
Pt6	661273.643	743273.718	323.211	0.011	0.024	RR	
Pt7	661277.000	743301.403	321.756	0.010	0.019	RL	
Pt8	661283.448	743298.036	321.695	0.011	0.023	RR	
Pt9	661279.788	743298.909	321.430	0.010	0.020	C	0+050
Pt10	661293.697	743324.028	320.848	0.010	0.018	RR	

The assessment revealed a mean Horizontal Root Mean Square (HRMS) value of 0.011 meters (equivalent to 11 millimeters) and a mean Vertical Root Mean Square (VRMS) value of 0.017 meters (17 millimeters). Notably, the calculated mean HRMS value aligns with the prescribed limiting RMSE of 0.0125 meters for Class 1 planimetric accuracy standards as delineated by the Federal Geographical Data Committee (1998). Similarly, the VRMS value falls within the accuracy requirement for well-defined points, specifically for a target contour interval of 0.1 meters, resulting in a limiting RMSE value of 0.03 meters according to Guyer (2017).

This comprehensive analysis underscores the dependability and suitability of the acquired data for endeavors demanding high precision, such as road corridor design. The longitudinal profile of the road was formulated utilizing measurements from the road center points. This profile measurement facilitated the determination of ground elevations and enabled the creation of a road profile view. This view serves as a foundational component in the development of longitudinal slope and vertical curve designs for the designated route.

4.2 Using an Unmanned Aerial Vehicle for the road corridor survey

After undertaking the aerial survey, an Orthomosaic of the area was generated. It showed the road corridor as well as features around the road corridor. It was exported in the GeoTiff format, a file format for storing geographic metadata that identifies the imagery's location in space and LZW compression. Figure 4 shows the orthomosaic of the study area obtained from the UAV survey. Field data acquired using the aerial survey method is tabulated in Table 3. It comprises the coordinates, elevations, chainages, and the respective descriptions.

In addition to the orthomosaic, a Digital Elevation Model of the road corridor and its surroundings was also built as seen in Figure 5. It was the source from which raster values of points to be used for road design were extracted. The elevation model has a minimum elevation of 304.324m and a maximum elevation of 344.914 m. It was exported in GeoTIFF format and has LZW compression. The lighter areas show places of high elevations, and the darker areas show places of lower elevations.

Elevations derived from ground surveying were supplemented by those extracted from the Digital Elevation Model (DEM) resulting from the Aerial Surveying. This amalgamation served as the foundation for computing the Root Mean Square Error (RMSE) discrepancies. A representative subset of these points and their corresponding extracted elevations is presented in Table 3.

Illustrating the long-term road profile, Figure 6 presents the results of this integration, showing the road corridor's elevation changes based on the UAV aerial survey data.

The accuracy of the orthomosaic and Digital Elevation Model was verified by a Root Mean Square Error of 0.028 during the georeferencing of the photos used to create them. This confirms that the aerial survey meets the standards outlined by the American Society for Photogrammetry and Remote Sensing (ASPRS) for Class 1 accuracy at a 0.1-meter contour interval, as noted by Guyer (2017).

The longitudinal profile delivers crucial insights, revealing segments of elevated terrain juxtaposed with lower sections along the road corridor. This information not only informs the determination of parameters pertinent to vertical curves but also guides the selection of the road's design speed.

Figure Error! No text of specified style in document.. Orthomosaic obtained from processing the data from the Aerial Survey

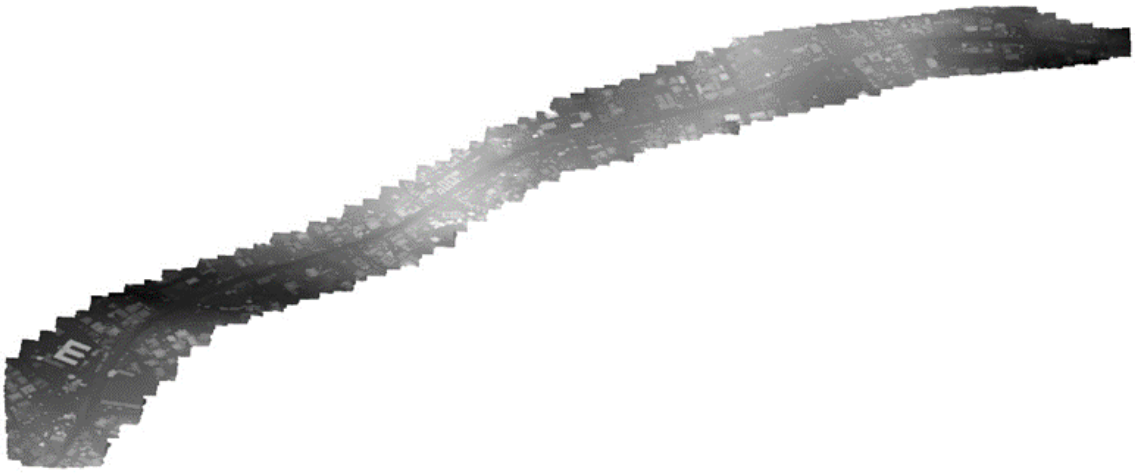

Figure 5. Digital Elevation Model

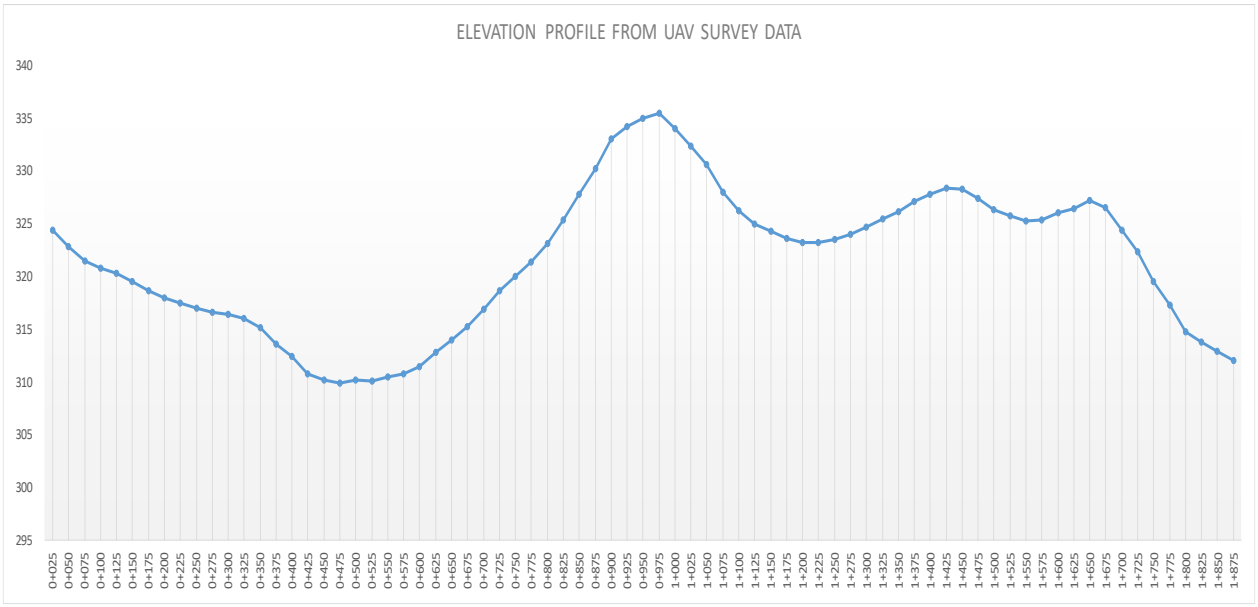

Figure 6. Longitudinal Profile from the UAV survey

Table 3. Sample of field data using the Aerial survey method

Point	Easting	Northing	Elevations (Z)	D	Chainage
Pt1	661257.545	743251.427	324.052	RL	
Pt2	661261.292	743249.590	324.386	C	0+025
Pt3	661264.438	743247.948	324.644	RR	
Pt4	661266.774	743276.205	323.104	RL	
Pt5	661269.404	743275.140	322.796	C	0+050
Pt6	661273.643	743273.718	323.290	RR	
Pt7	661277.000	743301.403	322.062	RL	
Pt8	661283.448	743298.036	321.933	RR	
Pt9	661279.788	743298.909	321.451	C	0+075
Pt10	661293.697	743324.028	320.893	RR	
Pt11	661290.801	743325.112	320.780	C	0+100
Pt12	661287.404	743326.397	320.870	RL	
Pt13	661297.892	743352.068	320.422	RL	
Pt14	661301.794	743349.639	320.242	C	0+125
Pt15	661307.649	743346.801	320.183	RR	
Pt16	661314.904	743373.192	319.798	RR	
Pt17	661311.182	743374.128	319.493	C	0+150
Pt18	661306.690	743375.192	319.159	RL	
Pt19	661314.580	743401.307	318.392	RL	
Pt20	661318.734	743400.023	318.595	C	0+175
Pt21	661323.192	743398.890	318.617	RR	
Pt22	661331.014	743424.403	318.094	RR	
Pt23	661327.548	743424.705	317.974	C	0+200
Pt24	661321.756	743426.126	317.970	RL	
Pt25	661330.274	743452.165	317.526	RL	
Pt26	661334.430	743451.386	317.464	C	0+225
Pt27	661338.734	743450.759	317.632	RR	
Pt28	661346.986	743476.531	329.414	RR	
Pt29	661341.508	743477.904	316.962	C	0+250

4.3 Comparing the data from both Survey methods

In pursuit of analyzing the disparities between data collected from ground surveying and UAV survey methods, a thorough analysis was performed. Ground Control Points (GCPs) were strategically used as reference points in this process. Table 4 shows the GCP coordinates obtained through RTK GPS observations alongside those extracted from the UAV dataset.

The topographic features of these GCPs were initially collected using on-site GNSS RTK GPS measurements. Additionally, the GCP locations were carefully recorded through aerial surveys using UAV technology. The elevation data associated with the GCPs were also derived from aerial imagery. This comprehensive approach ensured the collection of accurate data for assessing precision and conducting comparative analysis, summarized in Table 5.

The Root Mean Square Errors (RMSEs) calculated were 0 0.025 meters, 0 041 meters, and 0 057 meters for the Eastings, Northings, and Elevations, respectively. These values indicate a centimeter-scale deviation between the data from the two different surveying methods. This notably demonstrates UAV technology's ability to gather road topographic data suitable for design work. To visually compare the elevation differences between ground survey data and UAV survey data, longitudinal profiles were created from both datasets and overlaid, as shown in Figure 7. The red line represents the profile from UAV survey data, while the blue line shows the RTK GPS survey data. The positional accuracy of the datasets was also checked by overlaying the road corridor from each survey method, revealing no significant shifts in the corridor's location, as seen in Figure 8.

For position validation, the map of the ground-surveyed road corridor was superimposed onto the orthomosaic of the study area, as depicted in Figure 9, to confirm that there were no notable differences in their spatial alignment. To provide a thorough overview, cross sections at various chainages along the road were generated using data from both ground and

aerial surveys. Figures 10 to 13 display these cross-section overlays, showing consistency between the ground and aerial survey data at different points. To quantify the deviations in coordinates and elevations, errors were systematically calculated with the following formulas: $\Delta X = X\,2 - X\,1$, $\Delta Y = Y\,2 - Y\,1$, $\Delta Z = Z\,2 - Z\,1$.

Table 4. GCP checkpoints for RTK and UAV

	checkpoints from ground survey			**checkpoints from UAV survey**		
	X1	Y1	Z1	X2	Y2	Z2
GCP1	661257.399	743269.912	323.726	661257.3989	743269.9108	323.82272
GCP2	661369.874	743569.094	316.016	661369.9054	743569.0752	315.95026
GCP3	662638.808	744365.51	327.01	662638.7924	744365.5642	326.91852
GCP4	662752.049	744382.102	323.992	662752.0363	744382.0172	323.96448
GCP5	662856.832	744398.75	317.038	662856.8033	744398.7822	316.99573
GCP6	662446.75	744219.437	328.796	662446.7399	744219.4283	328.72522
GCP7	662283.37	744184.588	324.872	662283.3899	744184.5641	324.83768
GCP8	662066.36	744079.884	326.684	662066.4005	744079.9028	326.67126
GCP9	661904.983	743955.469	335.264	661904.9969	743955.4631	335.25256
GCP10	661789.092	743854.156	324.292	661789.0943	743854.1664	324.27112
GCP11	661607.69	743742.971	312.551	661607.7402	743742.8976	312.48749

Table 5. Calculation of Root Mean Square Error (RMSE)

	ΔX	ΔY	ΔZ	**(ΔX)²**	(ΔY)²	(ΔZ)²
GCP1	5.5659E-05	0.001238088	-0.09672	3.09792E-09	1.53E-06	0.009355
GCP2	-0.03143115	0.018842205	0.06574	0.000987917	0.000355	0.004322
GCP3	0.015588511	-0.05418884	0.09148	0.000243002	0.002936	0.008369
GCP4	0.012670815	0.084846407	0.02752	0.00016055	0.007199	0.000757
GCP5	0.028710124	-0.03216216	0.04227	0.000824271	0.001034	0.001787
GCP6	0.010059935	0.008665357	0.07078	0.000101202	7.51E-05	0.00501
GCP7	-0.01990213	0.023914653	0.03432	0.000396095	0.000572	0.001178
GCP8	-0.04051246	-0.01877178	0.01274	0.001641259	0.000352	0.000162
GCP9	-0.01390027	0.005942056	0.01144	0.000193218	3.53E-05	0.000131
GCP10	-0.00231333	-0.01036027	0.02088	5.35148E-06	0.000107	0.000436
GCP11	-0.05018703	0.07344603	0.06351	0.002518738	0.005394	0.004034
Total				0.007071606	0.018063	0.03554
RMSE				0.025355	0.040523	0.056841

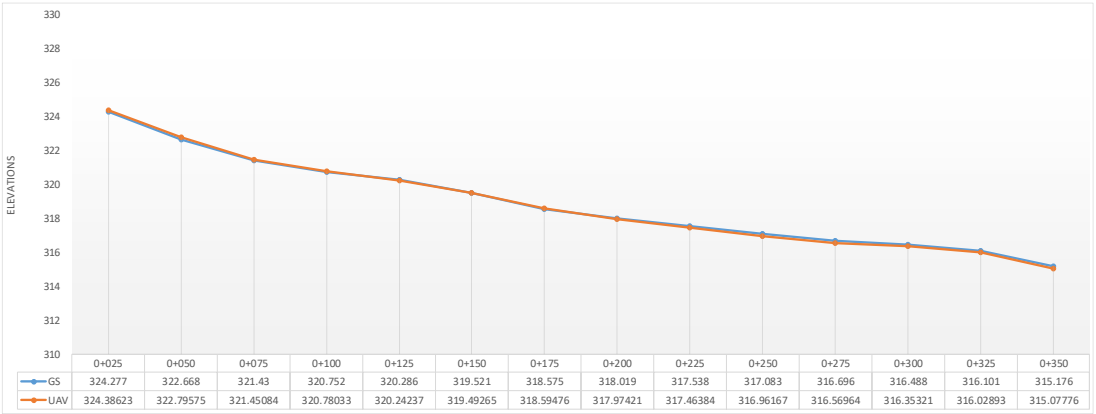

Figure 7. Longitudinal Profile from ground surveying superimposed on the longitudinal profile from the aerial survey

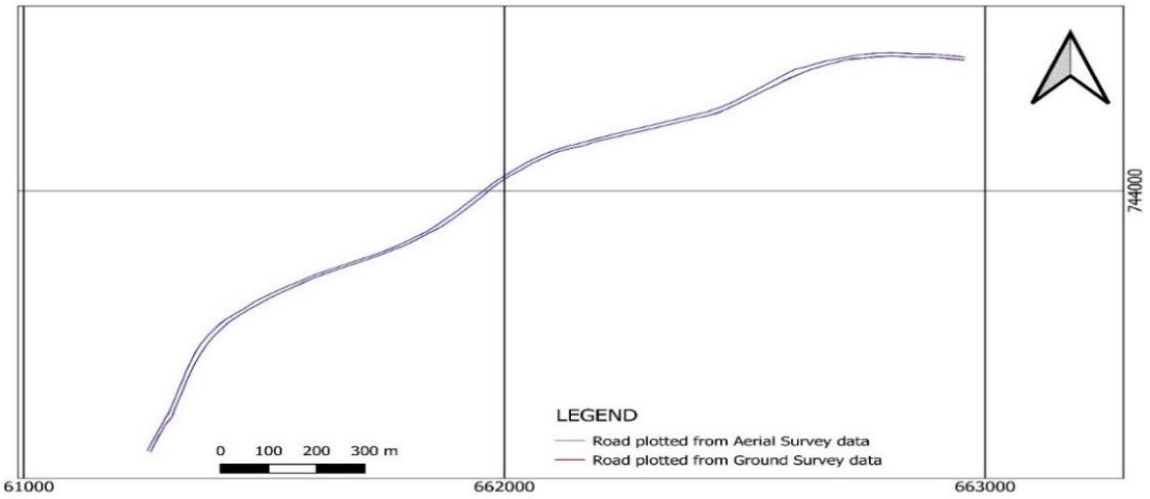

Figure 8. Map showing the superimposed road corridors

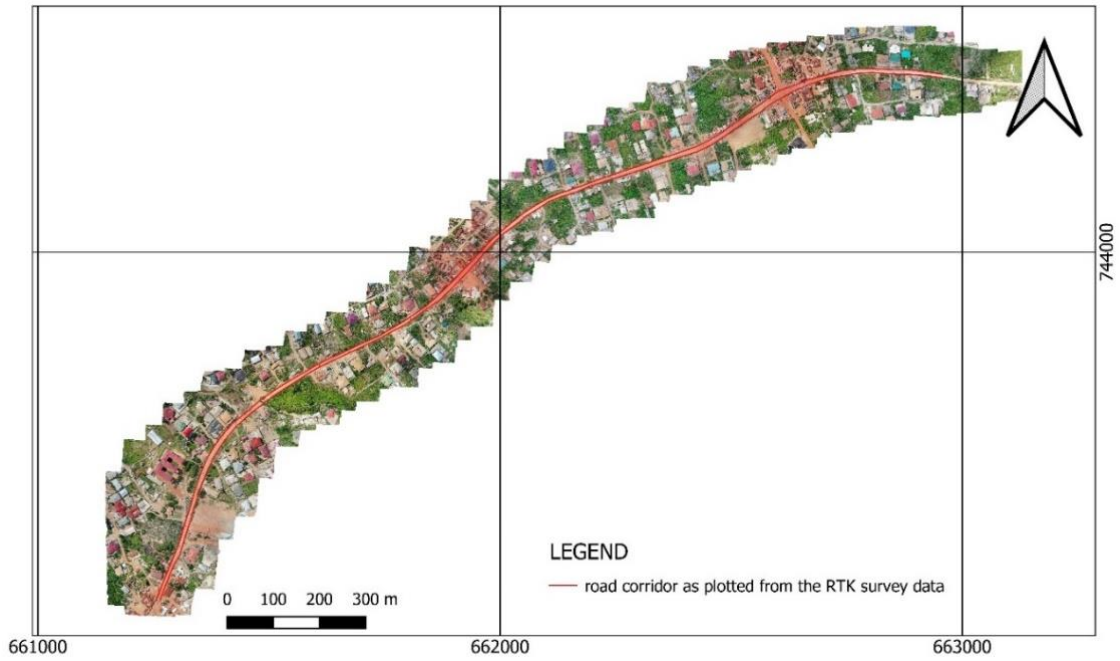

Figure 9. Map showing the road corridor from ground surveying superimposed on the generated orthomosaic

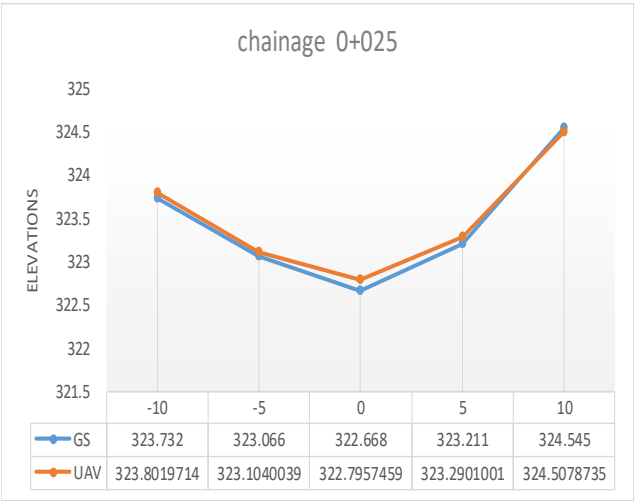

Figure 10. Cross section at chainage 0+025

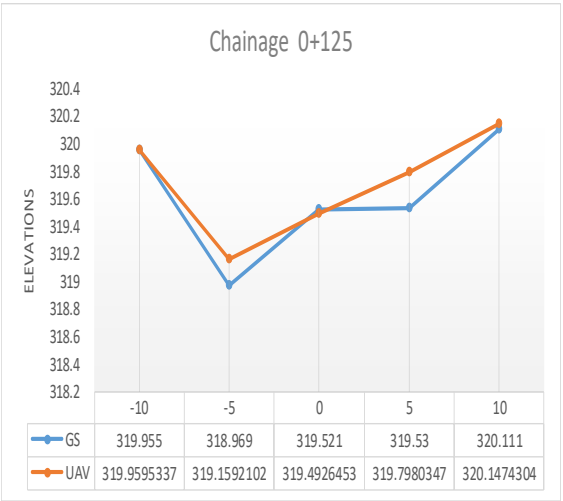

Figure 11. Cross section at chainage 0+125

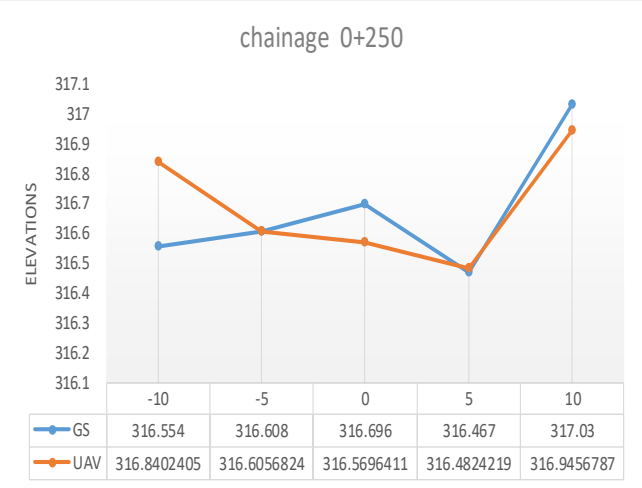

Figure 12. Cross section at chainage 0+250

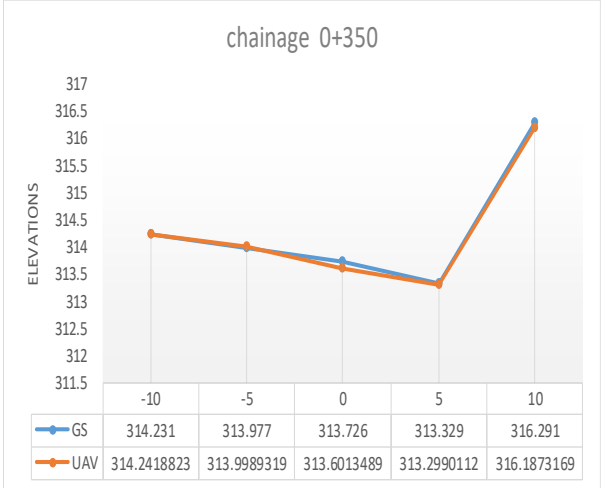

Figure 13. Cross section at chainage 0+350

Results from the longitudinal profiles, cross sections, and statistical performance evaluation were compared to assess the survey's accuracy and the potential use of UAVs for surveys. Elevations of detailed points obtained using the RTK GPS method were determined through trilateration with an accuracy of about 1cm. Since the RTK GPS method is the most precise, it served as the standard for comparing results from the UAV survey. The comparison of longitudinal profiles is shown in Figure 74.6. 6, while the cross-sectional comparisons at different chainages between UAV and GPS RTK measurements are presented in Figures 10 through 1327. The longitudinal profile highlights areas of higher and lower elevations along the road corridor. It was generated at 25-meter chainage intervals to capture detailed topographic information for design purposes. The profile helps determine parameters for vertical curves and aids in selecting appropriate design speeds for the road. Additionally, it identifies areas needing cut and fill. Slight deviations were observed between the superimposed profiles from both methods. Cross sections at various chainages along the road were created using data from ground and aerial surveys to compare the datasets. These sections were generated at 10-meter intervals from the centerline at 5 5-meter steps to record sufficient topographic data for design. They show the width of the road, side slopes of cuttings and embankments, road shoulders, and the carriageway camber. Most sections exhibited minor differences between the superimposed data from the two methods. The cross-sectional measurements also help determine elevation points in the pile at the midline topography for embankment earthwork calculations and construction side stakes (Wang and Hu, 2013). To evaluate the accuracy of the methods used, a statistical error analysis was conducted. The indicators included the arithmetic mean error (AME), arithmetic mean square error (AMSE), maximum and minimum residuals (rmin and rmax), and arithmetic standard deviation (ASD). Their mathematical expressions are provided by Equations 1 through 5, respectively.

$$AME = \frac{1}{n}\sum_{i=1}^{n}(\alpha_i - \beta_i) \quad (1)$$

$$AMSE = \frac{1}{n}\sum_{i=1}^{m}\left(\alpha_i - \beta_i\right)^2 \quad (2)$$

$$r_{\max} = \alpha_i - \beta_i \quad (3)$$

$$r_{\min} = \alpha_i - \beta_i \quad (4)$$

$$ASD = \sqrt{\frac{1}{n-1}\sum_{i=1}^{n}\left(\mu - \bar{\mu}\right)^2} \quad (5)$$

where n is the total number of observations, αi and βi are observations from UAV and RTK GPS, respectively, μ denotes the residual between the measurements from UAV and RTK GPS, respectively, μ is the mean of the residual, and i is an integer varying from 1 to n. Comparatively, with reference to the centre line profile, elevations obtained from the UAV had a continuous value of similar deviations from that of the RTK GPS, with a mean deviation value of -0.0326m. The maximum calculated residual error was 0.12775m, whereas the minimum residual error achieved a value of -0.17635 m. The Arithmetic mean error (AME) and the Arithmetic mean standard error (AMSE) were 0.032m and 0.0795m, respectively. Furthermore, the Arithmetic standard deviation (ASD) between both survey methods achieved a value of 1.1615E-16 m. The statistical performance results achieved imply a very good compatibility of the UAV survey measurements with RTK GPS measurements. However, the accuracy of the average value of deviations of UAV survey measurements from RTK GPS measurements can further be improved by adjusting flight level, image overlaps, and ground sample distance (GSD), which has a high impact on the resolution definition.

5. Conclusions and Recommendations

This study conducted a thorough comparison between the use of Unmanned Aerial Vehicles (UAVs) and traditional ground survey methods, particularly Real-Time Kinematic GPS equipment, for topographic surveys of road corridors. The effective use of the Real-Time Kinematic GPS method allowed for precise topographic assessments of the road corridor, including collecting spot elevations and edge positions that are vital for roadway design. Additionally, UAV technology proved effective in road corridor topographic surveying. Aerial photographs captured by UAVs were converted into a Digital Elevation Model and an orthomosaic, accurately outlining the edges of the road corridor through digitization. Elevation data within the corridor was extracted from the Digital Elevation Model, enabling the creation of longitudinal and cross-sectional profiles essential for design planning.

A comparative analysis of datasets from both survey methods showed minimal differences. Overlaying the road corridors mapped from RTK GPS and aerial survey data confirmed their relative positional stability. Similarly, overlaying the longitudinal and cross-sectional profiles obtained from both methods showed negligible discrepancies.

The accuracy assessment resulted in a Root Mean Square Error (RMSE) of 0 0.025355 meters, 0 0.040523 meters, and 0 0.056841 meters in the X, Y, and Z directions, respectively. These results highlight the potential of UAVs to deliver precise topographic data comparable to that achieved through Real-Time Kinematic GPS, with the added benefit of faster data collection.

In this study, the ground survey method (RTK GPS) was employed, utilizing Global Navigation Satellite System (GNSS) signals with differential corrections to achieve accurate point positioning. Future research should expand this comparative approach by including various traditional ground survey techniques, such as total stations with a ± 0 001 m least count. Additionally, modern ground survey methods like mobile laser scanning systems, vehicle-mounted laser systems, and Ground Penetrating Radar (GPR) should be investigated for future road survey projects.

The UAV equipped with a camera sensor successfully carried out aerial surveys of the road corridor. Further research is recommended into emerging drone technologies, including UAVs integrated with LiDAR, thermal sensors, multispectral cameras, infrared radiometers, and GPR systems. These technologies have the potential to produce highly detailed and accurate 3D measurements, improving the depth and precision of topographic data. Embracing these cutting-edge technologies will undoubtedly advance the field of road surveying and open new possibilities for detail and accuracy in topographic data collection

Acknowledgement

The writers would like to acknowledge the valuable contributions of the reviewers who provided constructive criticism and feedback, which helped improve the quality of this writing. AI tools (Quillbot and Grammarly) helped us to refine the grammar and enhance the work's readability. CSIR-BRRI is also recognized for providing the necessary resources to support the research findings

References

Acheamfour, L. B., and J. Tetteh (2014). 2010 Population and Housing Census, District Analytical Report, Kumasi Metropolitan. Ghana Statistical Service. www.statsghana.gov.gh

Amoah, A. S., E. M. Jr. Osei, A. A. Duker, and K. N. Osei (2012). Modeling land use change for the Ejisu-Juaben district of Ghana. Journal of Geomatics, 6(1), 7-10.

Beshr, A. A. A., and I. M. Abo Elnaga (2001). Investigating the accuracy of digital levels and reflectorless total stations for purposes of geodetic engineering. Alexandria Engineering Journal, 50, 399–405. https://doi.org/doi:10.1016/j.aej.2011.12.004

Bouziani, M., K. Yousfi, K. Charafi, and E. M. Zidane (2010). Quality standards of road surveying in Morocco. Fig Congress, Facing the Challenges – Building the Capacity, Sydney, Australia, 11-16 April 2010.

Chio, S., and C. Chiang (2020). Feasibility Study Using UAV Aerial Photogrammetry for a Boundary Verification Survey of a Digitalized Cadastral Area in an Urban City of Taiwan, Remote Sensing, 12(10), 1682. https://doi.org/10.3390/rs12101682

Cho, J., J. Lee, and B. Lee (2022). Application of UAV Photogrammetry to Slope-Displacement Measurement, KSCE J Civ Eng 26, 1904–1913. https://doi.org/doi: 10.1007/s12205-021-1374-1

Dou, S.Q. and Ding, S.Y. (2020). Construction of Smart Community Based on GIS and TILT. Int. Arch. Photogramm. Remote Sens. Spatial Inf. Sci., XLII-3/W10, 547–554, https://doi.org/10.5194/isprs-archives-XLII-3-W10-547-2020.

Federal Geographical Data Committee. (1998). Geospatial Positioning Accuracy Standards Part 3 : National Standard for Spatial Data Accuracy. National Spatial Data Infrastructure, 28. http://www.fgdc.gov/standards/projects/FGDC-standards-projects/accuracy/part3/chapter3

Guan, H., J. Li, S. Cao, and Y. Yu (2016). Use of mobile LiDAR in road information inventory: A review. Int. J. Image Data Fusion, 7(3), 219–242.

Ivanova, E. and Masarova, J. (2013). Importance of Road Infrastructure in the Economic Development and Competitiveness. Economics and Management, 18 (2), 263-274. https://doi.org/10.5755/j01.em.18.2.4253

Julge, K., A. Ellmann, and R. Köök (2019). Unmanned Aerial Vehicle Surveying For Monitoring Road. The Baltic Journal of Road and Bridge Engineering, 14(1), 1–17.

Laurent, J., J. F. Hébert, D. Lefebvre, Y. Savard (2012). Using 3D laser profiling sensors for the automated measurement of road surface conditions. In

Proc. 7th RILEM Int. Conf. Cracking Pavements. Dordrecht, The Netherlands: Springer, 157–167.

Lavine, A., J. N. Gardner, and S. L. Reneau (2003). otal station geologic mapping: an innovative approach to analyzing surface-faulting hazards. Engineering Geology, 70, 71–91. https://doi.org/doi:10.1016/S0013-7952(03)00083-8

Lee, J. M., K. S. Min, W. K. Min, and H. Park (2020). A Study on the Actively Capture of Road Construction Information Using Spatial Analysis. Journal of the Korean Society of Cadastre, 36(2), 149–159.

Li, W., M. Burrow, N. Metje, and G. Ghataora (2020). Automatic Road Survey by Using Vehicle Mounted Laser for Road Asset Management. IEEE Access, 8(June), 94643–94653. https://doi.org/10.1109/ACCESS.2020.2994470

Ljutić, K., A. Deluka-Tibljaš, and S. Babić (2008). Mogućnosti unapređenja planiranja i projektiranja cesta uporabom računala,. Zbornik Radova Građevinskog Fakulteta Sveučilišta u Rijeci XI, 189–2005.

Mensah, C., J. Atayi, A. T. Kabo-bah, M. Švik, D. Acheampong (2018). Assessing the Impacts of Urbinization on the Climate of Kumasi. May 2020. https://doi.org/10.20944/preprints201809.0059.v1

Moser, V., I. Barišić, D. Rajle, and S. Dimter (2016). Comparison of different survey methods' data accuracy for road design and construction. CENTRA 2016 4th International Conference on Road and Rail Infrastructure, January 2017, 1–8.

Osei-Nuamah, I., and E K. Appiah-Adjei (2017). Hydrogeological Evaluation Of Geological Formations In Ashanti Region. Ghana. Journal of Science and Technology, 37(1), 34–50.

Osman, A., P. K. Karikari, E. L. K. Osafo, and V. Attoh-Kotoku (2018). Smallholder Urban Cattle Production : Prospects and Challenges in the Kumasi Metropolis and Asokore Mampong Municipality of the Ashanti Region of Ghana. Journal of Animal Science and Biotechnology, 9(January), 98–110.

Paar, R., A. Marendić, and M. Zrinjski (2010). Metoda određivanja visina kombinacijom GNSS-a i laserskog sustava. Ekscentar, 12, 64–68.

Pajares, G. (2015). Overview and current status of remote sensing applications based on unmanned aerial vehicles (UAVs). Photogrammetric Engineering & Remote Sensing, 81(4), 281–330. https://doi.org/https://doi.org/10.14358/PERS.81.4.281.

Papí Ferrando, J. F., B., Halleman, T., Antonissen, F., Falco, B., Vizcarra-Mir, and L. Dezes (2007). The Socio-Economic Benefits of Roads in Europe. European Union Road Federation. https://doi.org/10.5281/zenodo.12014367.

Park, J. K., and D. Y. Um (2019). Comparison of Accuracy and Characteristics of Digital Elevation Model by MMS and UAV. Journal of the Korea Academia-Industrial Cooperation Society, 20(11), 13–18.

Pryor, W. T. (2004). Introduction to Photogrammetry and Aerial Surveys.

Psarianos, B., and B. Nakos (2001). A Cost-Effective Road Surveying Method for the Assessment of Road Alignments. Proc. IV International Symposium Turkish-German Joint Geodetic Days, January.

Rizos, C. (2003). Network RTK Research and Implementation : A Geodetic Perspective Network RTK Research and Implementation - A Geodetic Perspective. Journal of Global Positioning Systems, 1(2), 144–150. https://doi.org/10.5081/jgps.1.2.144

Saadatseresht, M., A. H. Hashempour, M. Hasanlou (2015). UAV Photogrammetry : A Practical Solution For Challenging Mapping Projects. XL, 23–25. https://doi.org/10.5194/isprsarchives-XL-1-W5-619-2015

Shi, X., and B. Wang (2021). Application of New Surveying and Mapping Technology in the Construction of Smart City. E3S Web of Conferences, Vo. 236, 04031, 4–7.

Siebert, S., and J. Teizer (2014). Mobile 3D mapping for surveying earthwork projects using an Unmanned Aerial Vehicle (UAV) system. Automation in Construction, 41, 1–14. https://doi.org/doi: 10.1016/j.autcon.2014.01.004

Streiter, R., and G. Wanielik (2013). The road surveying system of the federal highway research institute - A performance evaluation of road segmentation algorithms. Advances in Radio Science, 11. https://doi.org/10.5194/ars-11-81-2013

Um, J. K., D. Yong, P. J. Kyu, and U. D. Yong (2021). Accuracy Analysis of Road Surveying and Construction Inspection of Underpass Section using Mobile Mapping System. Journal of the Korean Society of Surveying, Geodesy, Photogrammetry and Cartography, 39(2), 103–111. https://doi.org/10.7848/ksgpc.2021.39.2.103

Wang, L., and W. Hu (2013). Study and Application in Road Survey on CORS Technique. Procedia - Social and Behavioral Sciences 96, 1707–1711. https://doi.org/10.1016/j.sbspro.2013.08.193

Winter, H. De, M. Bassier, M. Vergauwen Automation of As-Built Models. XLVI(2), 7–8.

Zulkipli, M. A., and K. N. Tahar (2018). Multirotor UAV-Based Photogrammetric Mapping for Road Design. International Journal of Optics, 2018(1), 1871058. https://doi.org/10.1155/2018/1871058